MRS Singapore – ICMAT Symposia Proceedings

8th International Conference on Materials for Advanced Technologies

Design, Simulations, and Optimizations of Mid-infrared Multiple Quantum Well LEDs

Ying DING[a,*], Laura MERIGGI[a], Matthew STEER[a,d], Weijun FAN[b], Kirill BULASHEVICH[c], Iain THAYNE[a], Calum MACGREGOR[d], Charlie IRONSIDE[e], and Marc SOREL[a]

[a]University of Glasgow, Oakfiled Ave, Glasgow, G12 8LT, United Kingdom
[b]Nanyang Technological University, 50 Nanyang Ave, Singapore, 639798, Republic of Singapore
[c]STR Group, Inc. – Soft-Impact, Ltd., Engels Ave, 194156, St. Petersburg, Russian Federation
[d]Quantum Device Solutions, Science Park, G20 0SP, Glasgow, United Kingdom
[e]Curtin University, Wark Ave, WA6102, Perth, Australia

Abstract

We use eight-band k·p energy band structure model to help design novel GaInSb/AlGaInSb mid-infrared multiple quantum well (MQW) structures with an emitting mid-infrared waveband of 4-5 µm. Simulation results suggest that the number of quantum wells has little influence on the spontaneous emission rate and gain because of no strong coupling between quantum wells and they just simply follow scaling laws. The SiLENSe software module from STR-soft is used to investigate injection efficiency of the designed MQW structures. Simulation results indicate that the MQW structures offer better carrier confinement i.e. higher carrier injection efficiency compared with traditional bulk active regions which are currently used for mid-infrared LEDs and sensors. Experimental investigations show that the MQW LEDs with a seven wells structure show an increase of a factor 2 in wall plug efficiency and output power compared with conventional bulk LEDs at the same wavelength.

* Corresponding author. Tel.: +44-141-330-6022
  E-mail address: ying.ding@glasgow.ac.uk

1. Introduction

Semiconductor materials such as antimonides emitting in the 3-5 µm mid-infrared (MIR) band are of great interest for the development of a low-cost photonic technology for the next generation of miniature and energy-efficient CO, CO_2, CH_4 gas sensors [1]. A well-established and cost effective approach is to directly grow the antimonide-based epilayer on a GaAs substrate [[2]]. In addition, GaAs substrate has a higher thermal conductivity of 0.55 W cm^{-1} °C^{-1} compared with that of GaSb substrate of 0.32 W cm^{-1} °C^{-1}. A buffer (interfacial) layer, such as a GaSb layer, is grown on top of the GaAs substrate to accommodate the large lattice mismatch [[3-7]]. (Al)InSb/AlInSb single QW LEDs emitting at ~5 µm with similar or lower output power of their counterpart of InSb and AlInSb bulk LEDs have been reported [[3, 4]]. After that, AlInSb bulk LEDs with variant wavelengths ranging from 3.4 µm to 5.7 µm have been investigated as a function of aluminum concentration between 8.8% to 0% [[5]]. Recently, efficiency droop in InSb/AlInSb single QW LEDs emitting at ~5 µm was revealed as a function of temperature for devices containing three different quantum well widths and the amount of droop is greatest at low temperature for the widest QWs [[8]]. So far, standard epilayer designs for MIR type-I LEDs and photodiodes still employ a bulk active region in combination with a relatively wide bandgap barrier between the active region and p-doping layer to reduce carrier leakage [[1, 9-13]]. For MIR type-I QW emitters which would be potential candidates for replacing bulk emitters, only (Al)InSb/AlInSb single QW LEDs [[3, 4, 8, 14]] emitting at ~5 µm and GaInSb/AlGaInSb dual QW lasers [[6, 7, 15]] emitting at 3-4 µm at low temperatures have been experimentally investigated. More QW numbers with a better carrier confinement in MIR type-I QW emitters, especially operating at 4.3 µm, have not been studied. As we know, the carrier leakage and localized high carrier densities are important mechanisms to impair output light power in LEDs [[16, 17]]. In this work, we report on a theoretical and experimental investigation of RT operated LEDs based on type-I GaInSb/AlGaInSb MQW active regions as a means of reducing carrier leakage and carrier densities. The spontaneous emission of the MIR type-I GaInSb/AlGaInSb MQW active regions, carrier injection efficiency and carrier concentration distributions on the MQW active regions were investigated using an eight-band k·p model and the SimuLED software, respectively. Room temperature photoluminescence from a GaInSb/AlGaInSb MQW wafer confirms the accurate emission wavelength of 4.3 µm we expected from the MQW active regions. LED devices based on the MQW active regions with a seven wells structure were fabricated and measured as well as compared with LEDs with an optimized bulk active region emitting at 4.3 µm using the same geometry and fabrication process. The results confirm the theoretical predictions and indicate that, compared to bulk LEDs, MQW LEDs have double the output power and wall-plug efficiency (WPE).

2. Design and Simulations

2.1. MQW structure

The designed MQW structures are detailed in Table 1. The design included an optical waveguide with a MQW core region between top and bottom cladding arranged in a p-i-n configuration. We used $Al_{0.2}In_{0.8}Sb$ as the confinement and cladding layers and the designed MQW consisted of ≥3 15 nm $Ga_{0.177}In_{0.823}Sb$ quantum wells/20 nm $Al_{0.1}Ga_{0.088}In_{0.812}Sb$ quantum barriers instead of bulk material as the active region. The well and barrier materials are lattice matched to the $Al_{0.2}In_{0.8}Sb$ pseudo-substrate in order to achieve multiple quantum wells without residual strain accumulation. The center emission wavelength for all structures was designed at 4.3 µm for the absorption and detection of carbon dioxide. Relatively low doping concentrations were kept in the p-doped layers for the sake of low light absorption losses. The conventional bulk structure emitting at the same wavelength is shown in Table 2 as reference. The epilayers consist of a GaSb buffer layer, a 3-µm n-type doping layer, followed by a 1-µm undoped active layer and a 0.5-µm p-type layer. A 20-nm p-type $Al_{0.2}In_{0.8}Sb$ barrier layer was grown between the p−layer and active layer in order to reduce electron leakage [18]. Tellurium and beryllium are used for n-type and p-type dopants, respectively.

Table 1. MIR GaInSb/AlGaInSb MQW structure.

Thickness (nm)	Repeat	Material	x	y	Type	Conc. (cm^{-3})
200		$Al_xIn_{1-x}Sb$	0.2		p	1E+18
1000		$Al_xIn_{1-x}Sb$	0.2		p	5E+17
1000		$Al_xIn_{1-x}Sb$	0.2		p	3E+17
400		$Al_xIn_{1-x}Sb$	0.2		p	2E+17
500		$Al_{(x)}Ga_{(y)}In_{(1-x-y)}Sb$	0.1	0.088	i(n)	1E+16
20	≥3	$Al_{(x)}Ga_{(y)}In_{(1-x-y)}Sb$	0.1	0.088	i(n)	1E+16
15	≥3	$Ga_{(x)}In_{(1-x)}Sb$	0.177		i(n)	1E+16
500		$Al_{(x)}Ga_{(y)}In_{(1-x-y)}Sb$	0.1	0.088	i(n)	1E+16
4000		$Al_xIn_{1-x}Sb$	0.2		n	7E17
300		GaSb				
		GaAs Substrate				

Table 2. MIR bulk structure.

Thickness (nm)	Material	x	Type	Conc. (cm^{-3})
500	$Al_xIn_{1-x}Sb$	0.05	p	7E+17
20	$Al_xIn_{1-x}Sb$	0.2	p	7E+17
1000	$Al_xIn_{1-x}Sb$	0.05	i(n)	9E15
3000	$Al_xIn_{1-x}Sb$	0.05	n	7E17
300	GaSb			
	GaAs Substrate			

2.2. Eight-band k·p model and simulations

As a representative result, the simulated spontaneous emission rate spectra (including TE mode and TM mode) for a seven wells structure under the carrier density of 5×10^{17}/cm^3 at RT are shown in Fig. 1. The spectra under other carrier densities are similar to the spectra in Fig. 1 expect the different intensities (not shown here). The shape of spontaneous emission rate spectra here is similar to previously reported spectral emittance from a 20-nm InSb/$Al_{0.143}In_{0.857}Sb$ QW at 15 K which was also calculated by an eight-band k·p model of the energy band structure [14]. The predicted transition energy of the investigated MQW is about 280 meV, 290 meV under the carrier densities of 5×10^{17}/cm^3, 1×10^{18}/cm^3 which corresponding to emission wavelengths of 4.4 µm, 4.3 µm, respectively. Here, we assumed the carrier density in each QW is the same. Simulation results also suggest that the number (1, 5, 7, and 10) of QW has little influence on the spontaneous emission rate and gain because of the thick quantum barriers (QBs) between QWs and they just simply follow scaling laws. The interaction between QWs can be ignored in this case. Even so, reduced carrier densities in the MQW for the same driving current would be an effective means to reduce carrier leakage and Auger-recombination, which becomes more prevalent under a high injection condition [16].
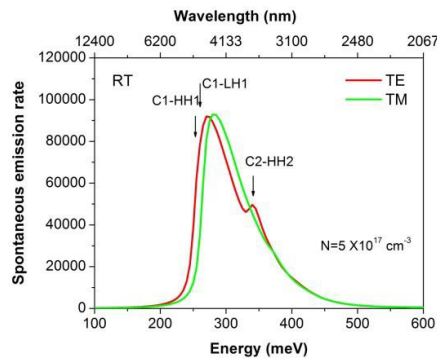

Fig. 1. Simulated spontaneous emission rate spectra of GaInSb/AlGaInSb MQW structure.

2.3. Injection efficiency simulations

The SimuLED software was used to simulate the band diagram and injection efficiency in MQW structures. The band diagrams of the MQW with seven wells and bulk structures under the bias voltage of 0.3 V are shown in Fig. 2 (a) and (b), respectively. From the band diagrams, the strong barriers can be seen in the MQW structure, whereas only a 20-nm quantum barrier whose thickness is limited by the material strain can be seen in the bulk structure. Further illustration of carrier leakage or injection efficiency for the MQW and bulk structures is shown in Fig. 3.
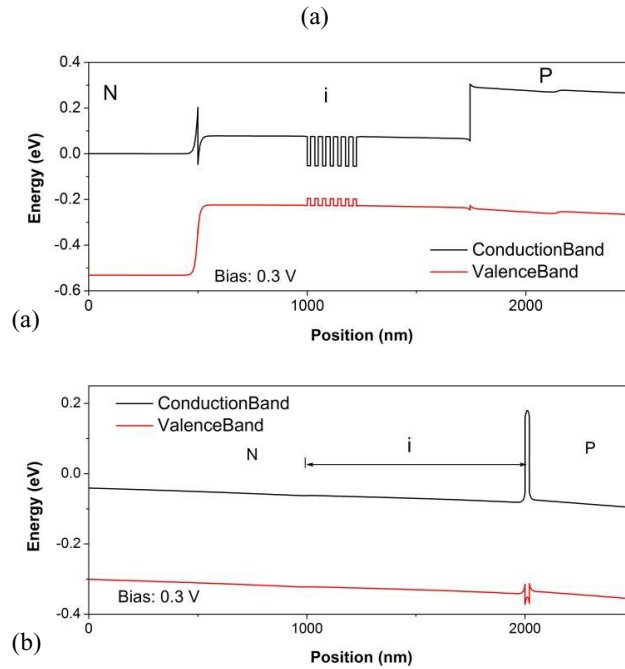
(a)

(a)

(b)

Fig. 2. Simulated energy-band diagrams of (a) GaInSb/AlGaInSb MQW and (b) bulk structure.
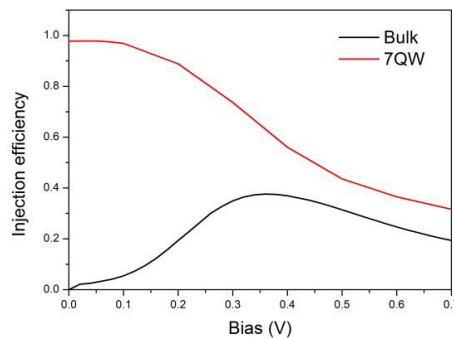

Fig. 3. Simulated injection efficiency in GaInSb/AlGaInSb MQW structure and bulk structure.

In addition, simulation results (Fig. 4) indicate that the injection efficiency can be further increased in the MQW structure by adding more quantum wells Increasing the QW number is also concluded to be beneficial to improve lateral current spreading for blue InGaN/GaN LEDs [19]. A systematically theoretical and experimental

investigation for the optimization of QW number in GaInSb/AlGaInSb MQW LEDs is underway and the results will appear elsewhere. It is also possible to further enhance the carrier confinement by increasing the energy band offset of the barriers, thereby further improving the injection efficiency.
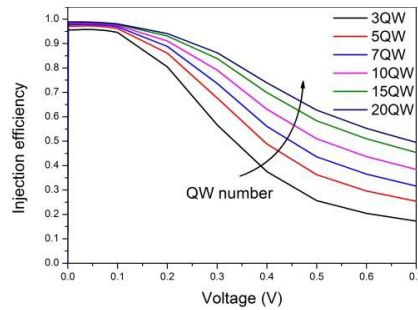

Fig. 4. Simulated injection efficiency in GaInSb/AlGaInSb MQW structure with different quantum well number.

3. Experimental results

3.1. Photoluminescence spectra

The epitaxial wafer with a seven GaInSb/AlGaInSb QWs structure depicted in Table 1 was grown on a semi-insulating GaAs substrate by molecular beam epitaxy. Photoluminescence (PL) spectra from MQW wafer was used to confirm the emission wavelength from the MQW active region. Before PL measurements, the MQW wafer was wet etched with a depth of about 2.4 µm in order to decrease the optical absorption caused by the thick upper confinement/cladding layers. A compact 300-mW diode-pumped solid state laser with a wavelength of 532 nm was used for excitation. The excitation beam was directed on the sample with a spot size of a few hundreds microns. The PL signal was collected from the same side of the sample using an off axis parabolic mirror, and focused onto the front entrance of a FTIR spectrometer containing a liquid-N_2-cooled InSb detector. The PL intensity is calibrated using a reference wafer before every measurement. The normalized PL spectra from the MIR MQW wafer and bulk wafer measured at RT are shown in Fig. 5. The expected emission wavelength of ~4.3 µm can be seen from the PL spectrum of MQW wafer, which is consistent with the simulated result. It is not easy to compare the PL intensities from MQW and bulk active region because of different layer structures above active regions leading to different optical absorption losses. Edge-excitation and edge-emission microphotoluminescence approach [20] may be tried in the future study in order to compare the PL intensities from samples with different upper confinement layers.
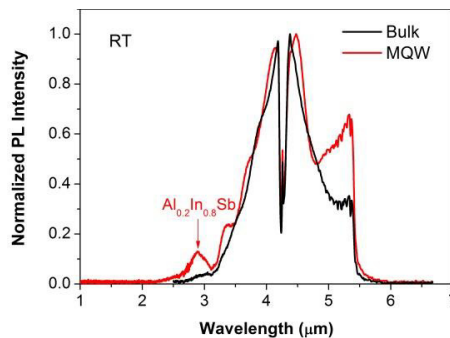

Fig. 5. Photoluminescence spectra of GaInSb/AlGaInSb MQW wafer and bulk wafer under the same excitation condition. The dip in the spectra at around 4.2-4.3 µm is due to CO2 absorption in the lab.
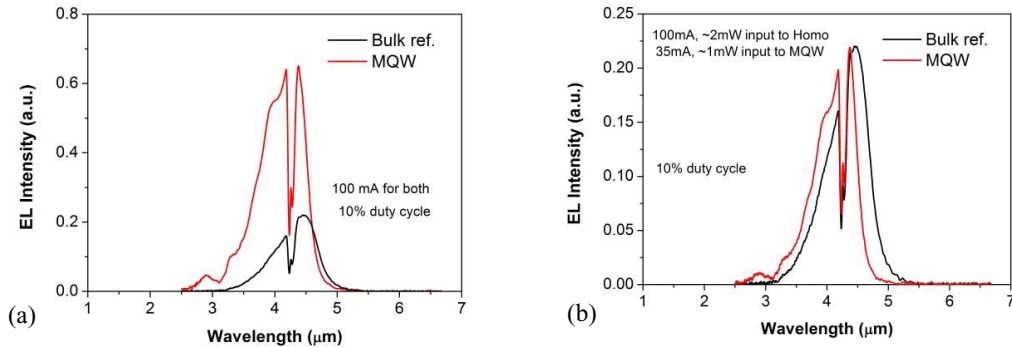
3.2. Electroluminescence spectra

Fig. 6. Comparison of electroluminescence spectra of GaInSb/AlGaInSb MQW LED and bulk LED, (a) under the same 100-mA pump current conditions; (b) with the same peak intensity. The dip in the spectra at around 4.2-4.3 µm is due to CO_2 absorption in the lab.

Further comparison of the electroluminescence (EL) spectra of the MQW LED and the bulk LED with pulsed current of 100 mA (1-kHz frequency and 10% duty cycle) at RT is shown in Fig. 6 (a). A 3-times improvement in integrated EL intensity can be observed from the MQW active region under the same operating current conditions, which corresponding to a 3-times improvement in the output power or internal quantum efficiency providing the light extraction efficiency for both is similar. The spectra in Fig. 6 (b) show that a similar peak intensity is emitted when an electrical power of 1 mW and 2-mW are injected in the MQW LED and the bulk LED, respectively, which manifests 2-times increase in WPE for MQW LED. The reason why the improvement in WPE is not as pronounced as that measured for the integrated EL intensity is due to the higher resistivity of the MQW epi-layers.

The results reported here were all obtained from top emission through the p-type cladding region. We plan further experiments to investigate edge emission and we expect edge emission to be improved by the optical waveguide structure.

4. Conclusions

In conclusion, MIR type-I LEDs based on GaInSb/AlGaInSb MQW active region have been theoretically and experimentally investigated. Simulation results show that a good wavelength control and a better carrier confinement in active region can be attained by including a MQW active region in the structure design. The experimental results indicate that the MQW LEDs with seven wells structure can provide a more than two-times increase in the output power and a two-times increase in the WPE compared to an optimized bulk LEDs, which is a significant breakthrough in 3-5 µm band type-I semiconductor LEDs. Furthermore, because of a large quantity of free parameters, such as QW number, compositions and thicknesses of QW and QB, strain, in the MQW LEDs design, the output power and WPE could be further improved through employing an optimized MQW structure in the near future.

Acknowledgements

References

[1] D. Gibson, C. MacGregor, A Novel Solid State Non-Dispersive Infrared CO2 Gas Sensor Compatible with Wireless and Portable Deployment, Sensors 13 (2013) 7079-7103.

[2] H. Hardaway, T. Ashley, L. Buckle, M. Emeny, G. Masterton, G. Pryce, in: Infrared Detector Materials and Devices, eds R.E. Longshore, S. Sivananthan (SPIE-INT SOC Optical Engineering, Bellingham, 2004).

[3] B.I. Mirza, G.R. Nash, S.J. Smith, M.K. Haigh, L. Buckle, M.T. Emeny, T. Ashley, InSb/AlxIn1-xSb quantum-well light-emitting diodes with high internal quantum efficiencies, Applied Physics Letters 89 (2006).

[4] G.R. Nash, M.K. Haigh, H.R. Hardaway, L. Buckle, A.D. Andreev, N.T. Gordon, S.J. Smith, M.T. Emeny, T. Ashley, InSb/AlInSb quantum-well light-emitting diodes, Applied Physics Letters 88 (2006).

[5] M.K. Haigh, G.R. Nash, S.J. Smith, L. Buckle, M.T. Emeny, T. Ashley, Mid-infrared AlxIn1-xSb light-emitting diodes, Applied Physics Letters 90 (2007).

[6] G.R. Nash, S.J. Smith, S.D. Coomber, S. Przeslak, A. Andreev, P. Carrington, M. Yin, A. Krier, L. Buckle, M.T. Emeny, T. Ashley, Midinfrared GaInSb/AlGaInSb quantum well laser diodes grown on GaAs, Applied Physics Letters 91 (2007).

[7] G.R. Nash, S.J.B. Przeslak, S.J. Smith, G. de Valicourt, A.D. Andreev, P.J. Carrington, M. Yin, A. Krier, S.D. Coomber, L. Buckle, M.T. Emeny, T. Ashley, Midinfrared GaInSb/AlGaInSb quantum well laser diodes operating above 200 K, Applied Physics Letters 94 (2009).

[8] G.R. Nash, B.I. Mirza, Efficiency droop in InSb/AlInSb quantum-well light-emitting diodes, Applied Physics Letters 102 (2013).

[9] L. Meriggi, M.J. Steer, M. Sorel, C.N. Ironside, I.G. Thayne, C. MacGregor, in: The European Conference on Lasers and Electro-Optics, (Munich Germany, 2013).

[10] G.R. Nash, T. Ashley, Reduction in Shockley–Read–Hall generation-recombination in AlInSb light-emitting-diodes using spatial patterning of the depletion region, Applied Physics Letters 94 (2009).

[11] G.R. Nash, H.L. Forman, S.J. Smith, P.B. Robinson, L. Buckle, S.D. Coomber, M.T. Emeny, N.T. Gordon, T. Ashley, Mid-Infrared AlxIn1-xSb Light-Emitting Diodes and Photodiodes for Hydrocarbon Sensing, Ieee Sensors Journal 9 (2009) 1240-1243.

[12] E.G. Camargo, K. Ueno, Y. Kawakami, Y. Moriyasu, K. Nagase, M. Satou, H. Endo, K. Ishibashi, N. Kuze, Miniaturized InSb photovoltaic infrared sensor operating at room temperature, Optical Engineering 47 (2008).

[13] K. Ueno, E.G. Camargo, T. Katsumata, H. Goto, N. Kuze, Y. Kangawa, K. Kakimoto, InSb Mid-Infrared Photon Detector for Room-Temperature Operation, Japanese Journal of Applied Physics 52 (2013).

[14] T.G. Tenev, A. Palyi, B.I. Mirza, G.R. Nash, M. Fearn, S.J. Smith, L. Buckle, M.T. Emeny, T. Ashley, J.H. Jefferson, C.J. Lambert, Energy level spectroscopy of InSb quantum wells using quantum-well LED emission, Physical Review B 79 (2009).

[15] M. Yin, G.R. Nash, S.D. Coomber, L. Buckle, P.J. Carrington, A. Krier, A. Andreev, S.J.B. Przeslak, G. de Valicourt, S.J. Smith, M.T. Emeny, T. Ashley, GaInSb/AlInSb multi-quantum-wells for mid-infrared lasers, Applied Physics Letters 93 (2008).

[16] G. Verzellesi, D. Saguatti, M. Meneghini, F. Bertazzi, M. Goano, G. Meneghesso, E. Zanoni, Efficiency droop in InGaN/GaN blue light-emitting diodes: Physical mechanisms and remedies, Journal of Applied Physics 114 (2013) -.

[17] J. Cho, E.F. Schubert, J.K. Kim, Efficiency droop in light-emitting diodes: Challenges and countermeasures, Laser & Photonics Reviews 7 (2013) 408-421.

[18] T. Ashley, C.T. Elliott, N.T. Gordon, R.S. Hall, A.D. Johnson, G.J. Pryce, Uncooled InSb/In1−xAlxSb mid-infrared emitter, Applied Physics Letters 64 (1994) 2433-2435.

[19] C.S. Xia, Z.M. Simon Li, Z.Q. Li, Y. Sheng, Z.H. Zhang, W. Lu, L.W. Cheng, Optimal number of quantum wells for blue InGaN/GaN light-emitting diodes, Applied Physics Letters 100 (2012) -.

[20] Y. Ding, W.J. Fan, B.S. Ma, D.W. Xu, S.F. Yoon, S. Liang, L.J. Zhao, M. Wasiak, T. Czyszanowski, W. Nakwaski, Microphotoluminescence investigation of InAs quantum dot active region in 1.3μm vertical cavity surface emitting laser structure, Journal of Applied Physics 108 (2010).